

## Electronic Supplementary Material

# Pd nano-catalyst supported on biowaste-derived porous nanofibrous carbon microspheres for efficient catalysis

Xianglin Pei<sup>1,2\*</sup>, Siyu Long<sup>1,4\*</sup>, Lingyu Zhang<sup>1,2</sup>, Zhuoyue Liu<sup>1,4</sup>, Wei Gong (✉)<sup>1,4</sup>, Aiwen Lei<sup>2</sup>, Dongdong Ye (✉)<sup>3</sup>

1 School of Materials and Architectural Engineering, Guizhou Normal University, Guiyang 550025, China

2 College of Chemistry and Molecular Sciences, Wuhan University, Wuhan 430072, China

3 School of Textile Materials and Engineering, Wuyi University, Jiangmen 529020, China

4 Guizhou Key Laboratory of Inorganic Nonmetallic Functional Materials, Guizhou Normal University, Guiyang 550025, China

E-mails: [gongw@gznu.edu.cn](mailto:gongw@gznu.edu.cn) (Gong W); [ydd@whu.edu.cn](mailto:ydd@whu.edu.cn) (Ye D)

## Experimental section

### Materials

Chitin was purchased from Zhejiang Golden Shell Biochemical Co., Ltd (Zhejiang, China). Palladium acetate (Pd(OAc)<sub>2</sub>, 99%, Beijing Bailing Wei Technology Co., Ltd), commercial 5 wt% Pd/C (Aladdin), nano-Pd powders (Aladdin), Span 85 (Aladdin), Tween 85 (Aladdin), and isooctane (AR, Tianjin Damao Chemical Reagent Factory) were used as received. All other reagents, such as methanol, acetone, hydrochloric acid, *etc.*, are obtained from various commercial resources and can be used without further purification. Methylene blue (MB), methyl red (MR), methyl orange (MO), rhodamine B (Rh B), congo red (CR), phenol red (PR) (Aladdin), benzaldehyde and benzaldehyde derivatives were supplied by Aladdin and could be used without further purification.

## **Characterization**

Scanning electron microscopy (SEM) images were observed by field emission scanning electron microscopy (FESEM, Zeiss SUPRA 55 Sapphire, Germany) at an accelerating voltage of 5 kV. Transmission electron microscopy (TEM) images were collected on a JEM-2010 (HT) electron microscope (JEOL, Japan) with an accelerating voltage of 200 kV. Before the TEM observation, we first grinded the sample thoroughly, then impregnated it with ethanol and dropped the suspension onto a copper grid. Infrared spectroscopy was carried out using a Fourier transform infrared (FT-IR) spectrometer (model IS5, Japan). Nitrogen physisorption measurements were recorded by a Micromeritics AsAp2020 (USA). X-ray photoelectron spectroscopy (XPS) was collected on a VG Multi Lab 2000 system with a monochromatic Al  $K\alpha$  X-ray source (Thermo Fisher scientific ESCALAB 250Xi, USA). X-ray diffractometer (XRD, S2, Rigaku, Japan). The content of palladium in the catalyst was determined by IRISIntrepidII (Thermo) inductively coupled plasma atomic emission spectrometry (ICP-OES, Shimadzu). GC yields were recorded with a Varian GC 3900 gas chromatography instrument with a FID detector. The degradation of dyes was tested by ultraviolet spectrophotometer (UV-2550, Shanghai Yuanxi Instrument Co., Ltd.).

## **Determination of Pd loading**

The obtained Pd/NCM catalyst (5~10 mg) was stirred in 120 °C nitric acid solution (8 mL) for 12 h, and then diluted with deionized water to 100 mL after the supported catalyst was soluble. Subsequently, the resulting solution was performed on an

ICP-OES (Prodigy 7, Leeman Labs Inc., U. S. A.), and the result showed that the Pd loading in Pd/NCM catalyst was 0.64 wt. %.

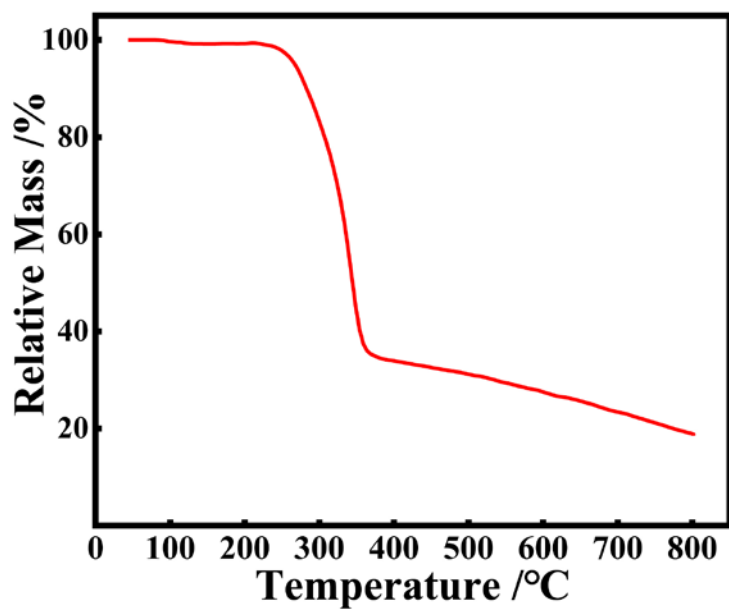


Figure S1. TG curves of the CM.

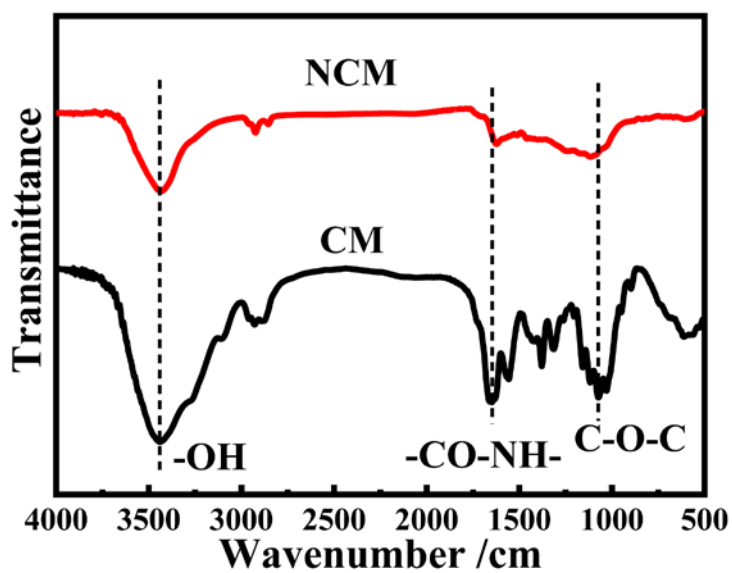
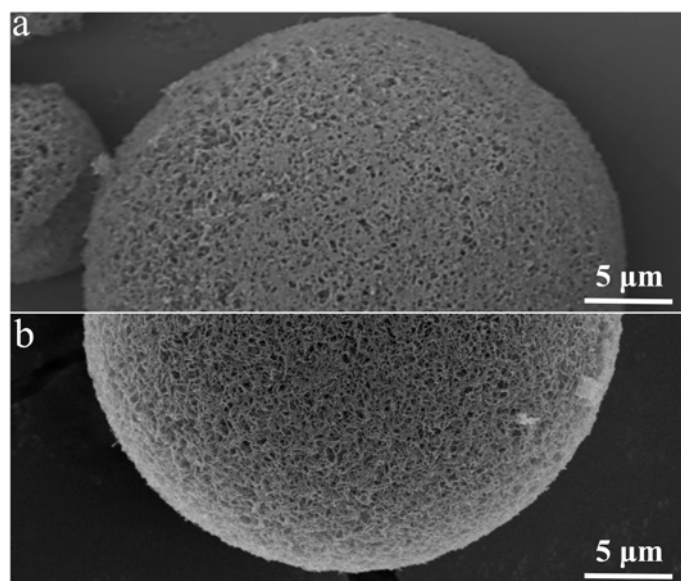
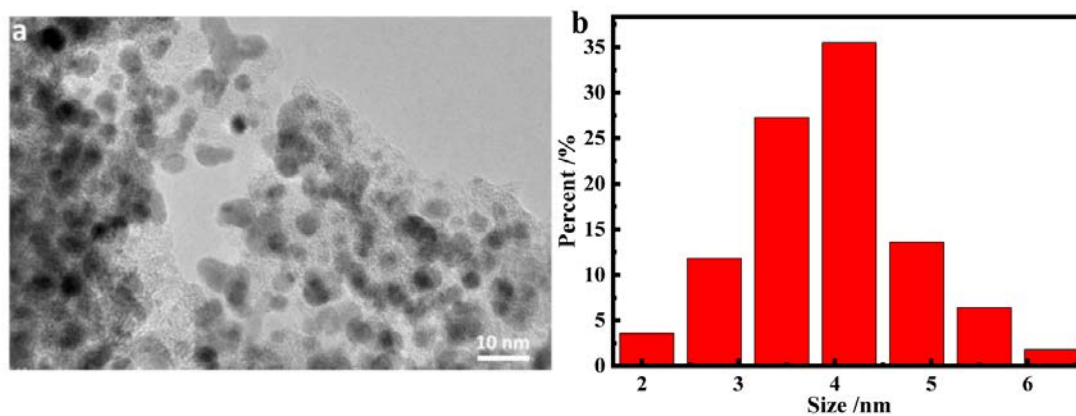


Figure S2. FT-IR spectra of the CM and NCM.



**Figure S3.** SEM images of the CM (a) and NCM (b).



**Figure S4.** TEM image of the commercial Pd/C (a), and size distribution of the Pd NPs (b).

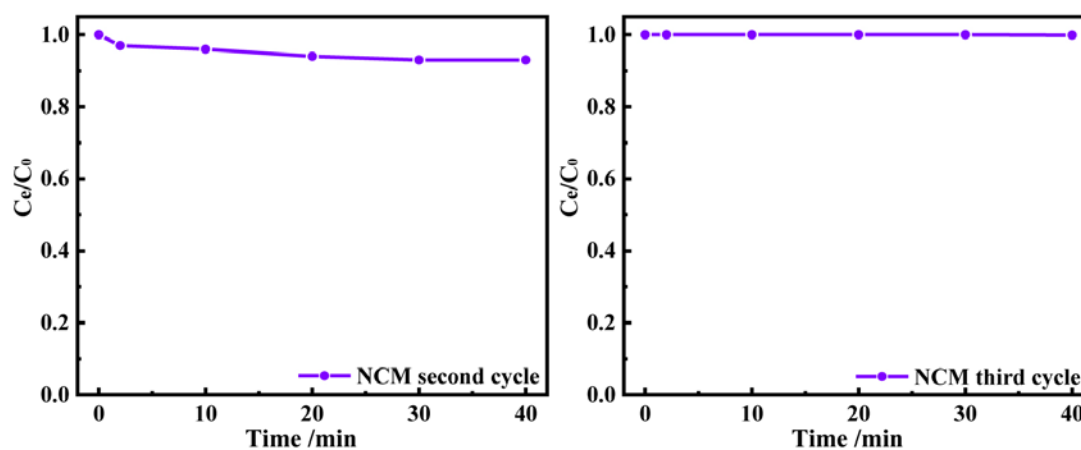


**Figure S5.** The degradation rate vs. reaction time plots for degradation of MB catalyzed by bare NCM in the second and third run.

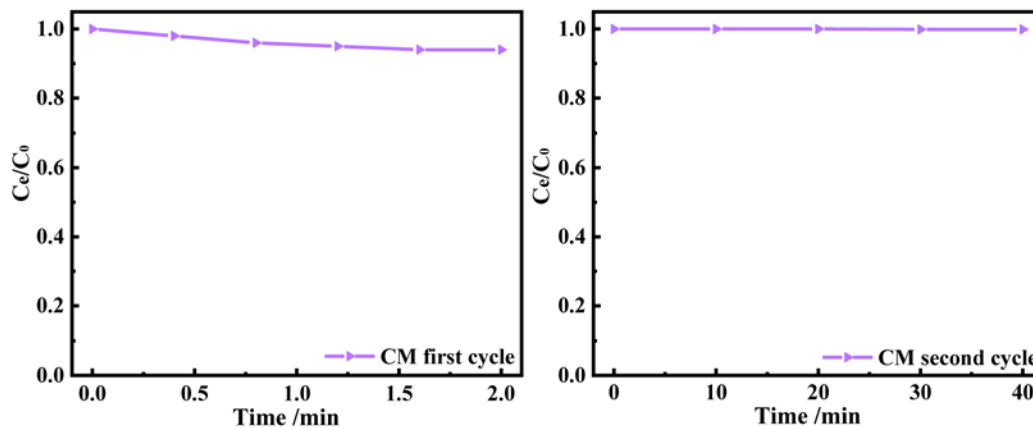


**Figure S6.** The degradation rate vs. reaction time plots for degradation of MB catalyzed by bare chitin (CM) in the first and second run.

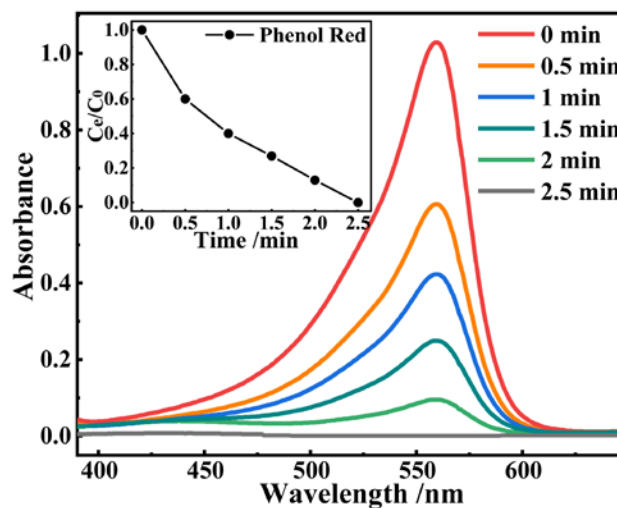


**Figure S7.** UV-visible absorption spectra with time for the degradation of PR catalyzed by Pd/NCM.

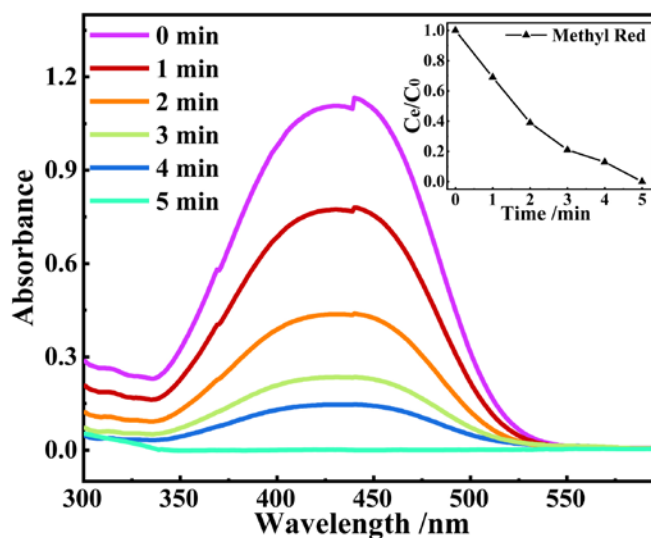


**Figure S8.** UV-visible absorption spectra with time for the degradation of MR catalyzed by Pd/NCM.

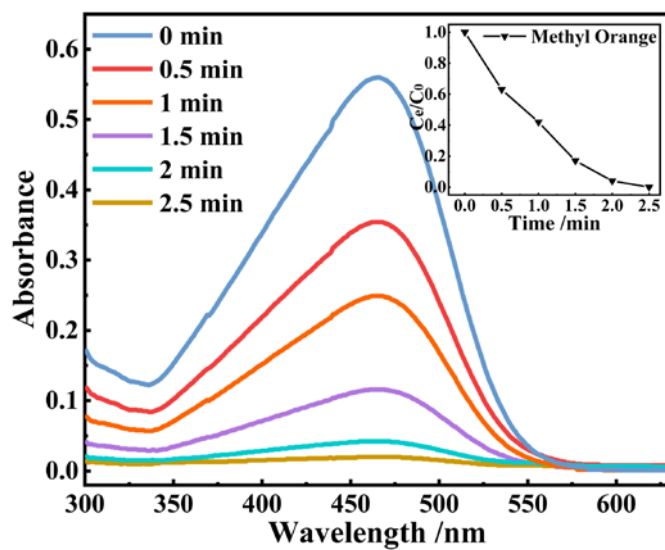


**Figure S9.** UV-visible absorption spectra with time for the degradation of MO catalyzed by Pd/NCM.

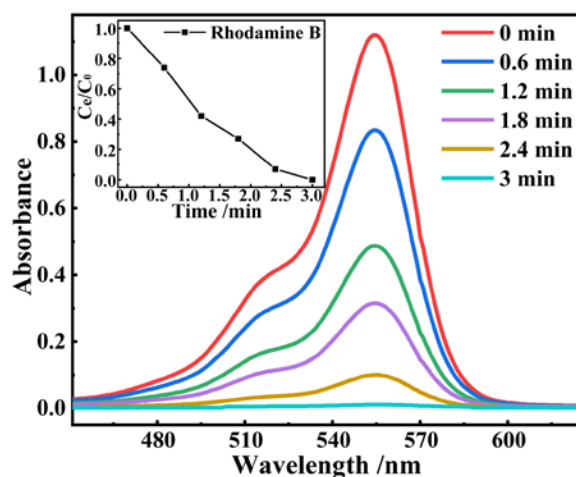


**Figure S10.** UV-visible absorption spectra with time for the degradation of Rh B catalyzed by Pd/NCM.

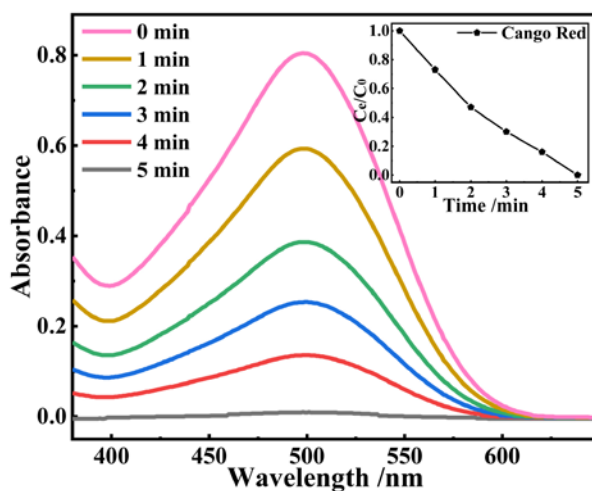


**Figure S11.** UV-visible absorption spectra with time for the degradation of CR catalyzed by Pd/NCM.

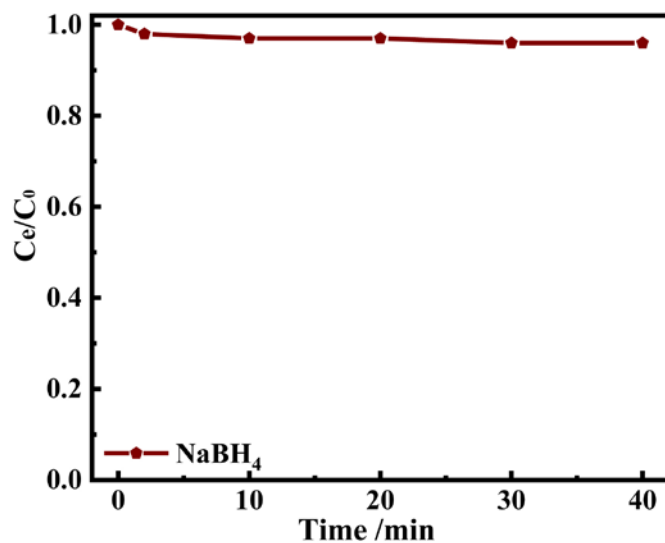


**Figure S12.** The degradation rate vs. reaction time plots for degradation of MB in the presence of  $\text{NaBH}_4$ .

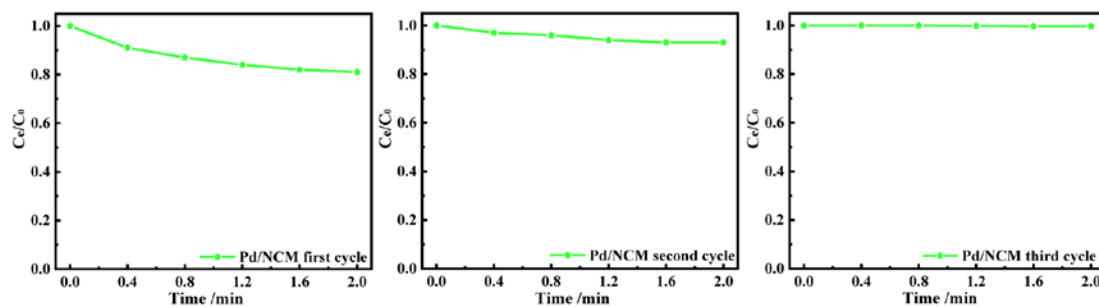


**Figure S13.** The degradation rate vs. reaction time plots for degradation of MB catalyzed by Pd/NCM without  $\text{NaBH}_4$  in the first, second, third run.

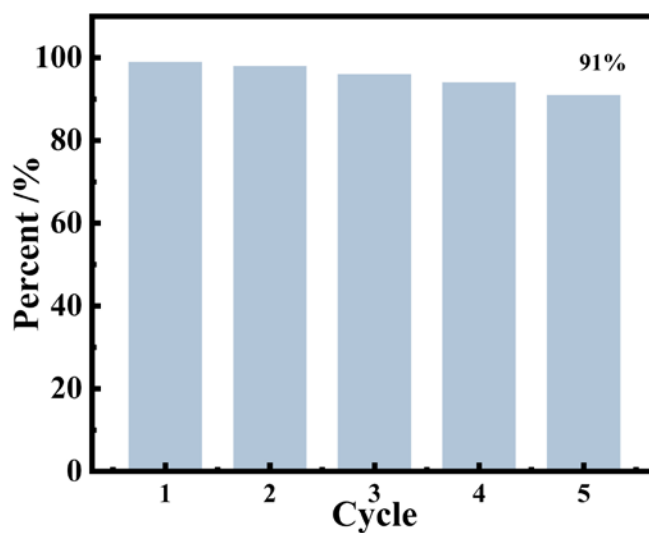


**Figure S14.** Cycle activity of Pd/NCM in 5 runs.

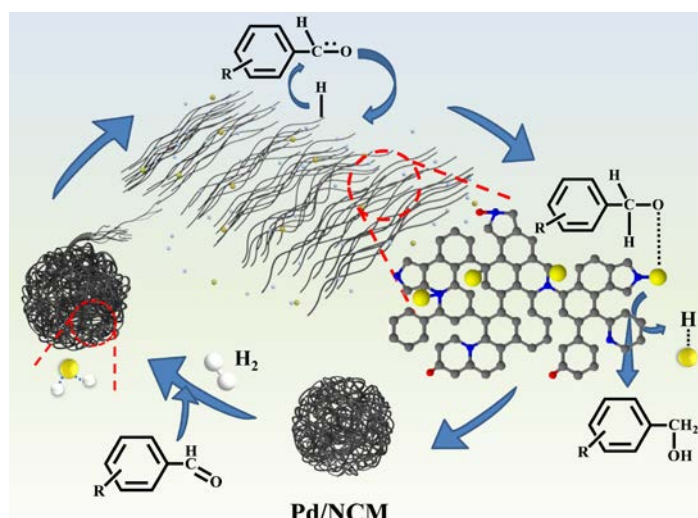


**Figure S15.** The mechanism for hydrogenation of aromatic aldehydes by Pd/NCM catalyst.

**Table S1.** Elemental analysis data of CM and NCM

Sample	C%	H%	N%	O%
CM	42.77	6.71	6.35	44.17
NCM	76.75	2.19	5.05	16.01

**Table S2.** TOF values of the Pd/NCM catalyst in common 6 dyes.

Dye	MB	PR	MR	MO	Rh B	CR
TOF(h <sup>-1</sup> )	1315.8	1052.6	30303.0	1052.6	869.5	526.3

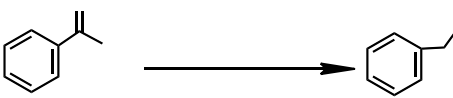
**Table S3.** Comparison of catalytic activity of dye degradation for Pd/NCM and reported catalysts.

Catalyst	Dye	Catalysis condition	Catalyst (mg)	Dye concentration (ppm)	Reaction time (min)	Degradation (%)	Rate constant (min <sup>-1</sup> )	Ref.
$\kappa$ -CG-s-Ag NPs	MB	RT, NaBH <sub>4</sub>	-	300.0	3.7	95.0	0.460	[1]
CoSiOx/PMS	MB	25°C, peroxymonosulfate	10	50.0	9.0	~98.0	0.386	[2]
SnO <sub>2</sub> NPs	MB	RT, 500 W mercury lamp ( $\lambda$ ~ 365 nm)	45	10.0	50.0	90.0	0.044	[3]
SnS <sub>2</sub> -SiO <sub>2</sub> @ $\alpha$ -Fe <sub>2</sub> O <sub>3</sub>	MB	RT, 0.06 W LED light ( $\lambda$ ~ 410 nm)	40	5.0	100.0	96.0	0.020	[4]
CdS/Cu <sub>7</sub> S <sub>4</sub> -5	MB	30°C, UV light	30	30.0	20.0	98.0	0.168	[5]
Ge/GeO <sub>2</sub>	MB	RT, In dark	-	1.6	60.0	96.0	0.077	[6]
Au-ZnO	MB	RT, UV light	-	0.03	60.0	98.0	-	[7]
Pd@chitosan	MB	RT, NaBH <sub>4</sub>	4	32.0	2.0	100.0	-	[8]
CS-La-GR composite	MB	RT, UV lamp ( $\lambda$ ~ 254 nm)	100	30.0	40.0	93.5	0.052	[9]



Au/CeO <sub>2</sub> -TiO <sub>2</sub>	MB	30°C, NaBH <sub>4</sub>	13	15.4	-	-	0.334	[11]
<b>Pd/NCM</b>	MB	RT, NaBH <sub>4</sub>	<b>1</b>	<b>31985.0</b>	<b>2.0</b>	<b>100.0</b>	<b>1.395</b>	<b>This work</b>
κ-CG-s-AgNPs	Rh B	RT, NaBH <sub>4</sub>	-	300.0	4.7	93.0	0.380	[1]
Ag <sub>2</sub> S-ZnS/cellulose	Rh B	27°C, 500 W tungsten halogen bulb	30	30.0	90.0	98.0	0.006	[10]
Au/CeO <sub>2</sub> -TiO <sub>2</sub>	Rh B	30°C, NaBH <sub>4</sub>	-	23.0	10.0	-	0.224	[11]
ZnIr-MOF-d <sub>0.3</sub>	Rh B	RT, visible light	10	50.0	30.0	~100	-	[12]
<b>Pd/NCM</b>	Rh B	RT, NaBH <sub>4</sub>	<b>1</b>	<b>47901.0</b>	<b>3.0</b>	<b>100.0</b>	<b>1.053</b>	<b>This work</b>
DLP-Au NPs	MO	RT, NaBH <sub>4</sub>	-	32.7	8.0	~100.0	0.102	[13]
Cu-NMOF/Ce-doped-Mg-Al-LDH	MO	RT, NaBH <sub>4</sub>	0.05	3273.3	1.0	-	1.86	[14]
Au/CB	MO	RT, NaBH <sub>4</sub>	10	160.0	4.0	-	1.29	[15]
Ag/TP	MO	RT, NaBH <sub>4</sub>	10	13.1	10.0	~100	-	[16]
<b>Pd/NCM</b>	MO	RT, NaBH <sub>4</sub>	<b>1</b>	<b>32733.0</b>	<b>2.5</b>	<b>100.0</b>	<b>1.581</b>	<b>This work</b>
DLP-Au NPs	CR	RT, NaBH <sub>4</sub>	-	7.0	10	~100	0.27	[13]
Au-ZnO	CR	RT, NaBH <sub>4</sub>	0.05	6966.8	1.0	-	2.76	[14]
Au/CB	CR	RT, NaBH <sub>4</sub>	10	160.0	15.0	-	0.365	[15]
Ag/TP	CR	RT, NaBH <sub>4</sub>	10	27.9	12.0	96.9	0.128	[16]
<b>Pd/NCM</b>	CR	RT, NaBH <sub>4</sub>	<b>1</b>	<b>69668.0</b>	<b>5.0</b>	<b>100.0</b>	<b>0.417</b>	<b>This work</b>

**Table S4.** Hydrogenation of benzaldehyde in various reaction conditions<sup>a</sup>



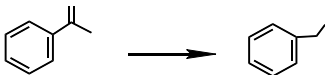
Entry	Catalyst	Solvent	Temperature (°C)	Catalyst (mol %)	Yield <sup>b</sup> (%)
1	Pd/NCM	PhMe	25	0.086	75
2	Pd/NCM	EtOAc	25	0.086	79
3	Pd/NCM	THF	25	0.086	12
4	Pd/NCM	H <sub>2</sub> O	25	0.086	87
5	Pd/NCM	DMF	25	0.086	Trace
6	Pd/NCM	IPA	25	0.086	54
7	Pd/NCM	MeOH	25	0.086	99
8	Pd/NCM	MeOH	45	0.086	97
9	Pd/NCM	MeOH	60	0.086	82
10	Pd/NCM	MeOH	90	0.086	34

11	Pd/NCM	MeOH	25	0.017	42
12	Pd/NCM	MeOH	25	0.043	81
13	Pd/NCM	MeOH	25	0.13	96
14	Pd/C	MeOH	25	0.13	37
15	Nano-Pd	MeOH	25	0.13	4
16	NCM	MeOH	25	-	0

<sup>a</sup>Reaction conditions: benzaldehyde (0.5 mmol), solvent (5 mL), and Pd catalyst (0.086 mol% [Pd], Pd: benzaldehyde), in 1 bar H<sub>2</sub> for 4 h.

<sup>b</sup>Yields of the products were determined using GC.

**Table S5.** Comparison of hydrogenation activity of benzaldehyde



Catalyst	Conditions	Catalyst (mg)	[Pd] (mol%)	Time (h)	T (°C)	Yield (%)	TOF (h <sup>-1</sup> )	Ref.
GO-Se-Pd	2-Propanol+KOH	10	0.25	3	45	97	129.3	17
Pd/N400-CNT	EtOH, 1 bar H <sub>2</sub>	94.1	0.35	0.83	45	96	330.5	18
Pd@HPC-DCD	H <sub>2</sub> O, 0.5 MPa H <sub>2</sub>	15	0.82	12	80	~100	10.2	19
Pd@N-C	MeOH, 5 bar H <sub>2</sub>	50	0.47	1	30	100	215	20
Pd@TP-POP	i-PrOH+KOH	10	-	3	80	98	-	21
Pd/GNP	<i>p</i> -xylene, 2 bar H <sub>2</sub>	15	0.10	5	50	~100	250	22
Pd/AC	cyclohexane, 15 bar H <sub>2</sub>	50-200	-	24	85	15	-	23
Pd/CNF	cyclohexane, 15 bar H <sub>2</sub>	50-200	-	24	85	16.8	-	23
Pd/O-CNT	EtOH, 1 bar H <sub>2</sub>	94.1	0.35	0.83	45	27	92.9	18
Pd/NCM	MeOH, 1 bar H <sub>2</sub>	~7.2	0.086	4	25	99	287.8	This work

## Reference

1. Pandey S, Do J Y, Kim J, Kang M. Fast and highly efficient catalytic degradation of dyes using kappa-carrageenan stabilized silver nanoparticles nanocatalyst. *Carbohydrate Polymers*, 2020, 230: 115597
2. Zhu Z S, Yu X J, Qu J, Jing Y Q, Abdelkrim Y, Yu Z Z. Preforming abundant surface cobalt hydroxyl groups on low crystalline flowerlike Co<sub>3</sub>(Si<sub>2</sub>O<sub>5</sub>)<sub>2</sub>(OH)<sub>2</sub> for enhancing catalytic degradation performances with a critical nonradical reaction. *Applied Catalysis B-Environmental*, 2020, 261: 118238
3. Li Y Y, Yang Q M, Wang Z M, Wang G Y, Zhang B, Zhang Q, Yang D F. Rapid fabrication of SnO<sub>2</sub> nanoparticle photocatalyst: computational understanding and

- photocatalytic degradation of organic dye. *Inorganic Chemistry Frontiers*, 2018, 5(12): 3005-3014
4. Balu S, Uma K, Pan G T, Yang C K, Ramaraj S K. Degradation of methylene blue dye in the presence of visible light using  $\text{SiO}_2@ \alpha\text{-Fe}_2\text{O}_3$  nanocomposites deposited on  $\text{SnS}_2$  flowers. *Materia*, 2018, 11(6): 1030
  5. Wan M L, Cui S Z, Wei W T, Cui S W, Chen K Y, Chen W H, Mi L W. Bi-component synergic effect in lily-like  $\text{CdS}/\text{Cu}_7\text{S}_4$  QDs for dye degradation. *RSC Advances*, 2019, 9(5): 2441-2450
  6. Shinde S, Nanda K. Photon-free degradation of dyes by  $\text{Ge}/\text{GeO}_2$  porous microstructures. *ACS Sustainable Chemistry & Engineering*, 2019, 7: 6611-6618
  7. Brahiti N, Hadjersi T, Amirouche S, Menari H, ElKechai O. Photocatalytic degradation of cationic and anionic dyes in water using hydrogen-terminated silicon nanowires as catalyst. *International Journal of Hydrogen Energy*, 2018, 43(24): 11411-11421
  8. Sargin I, Baran T, Arslan G. Environmental remediation by chitosan-carbon nanotube supported palladium nanoparticles: conversion of toxic nitroarenes into aromatic amines, degradation of dye pollutants and green synthesis of biaryls. *Separation And Purification Technology*, 2020, 247: 116987
  9. Sirajudheen P, Meenakshi S. Facile synthesis of chitosan- $\text{La}^{3+}$ -graphite composite and its influence in photocatalytic degradation of methylene blue. *International Journal of Biological Macromolecules*, 2019, 133(15): 253-261
  10. Kumar T K M P, Kumar S K A. Visible-light-induced degradation of rhodamine B by nanosized  $\text{Ag}_2\text{S}-\text{ZnS}$  loaded on cellulose. *Photochemical & Photobiological Sciences*, 2019, 18(1): 148-154
  11. Saikia P, Miah A T, Das P P. Highly efficient catalytic reductive degradation of various organic dyes by  $\text{Au}/\text{CeO}_2\text{-TiO}_2$  nano-hybrid. *Journal of Chemical Sciences*, 2017, 129: 81-93
  12. Fan K, Nie W, Wang L, Liao C. Defective metal-organic frameworks incorporating iridium-based metalloligands: sorption and dye degradation properties. *Chemical*, 2017, 23(27): 6615-6624

13. Umamaheswari C, Lakshmanan A, Nagarajan N S. Green synthesis, characterization and catalytic degradation studies of gold nanoparticles against congo red and methyl orange. *Journal of Photochemistry and Photobiology B-Biology*, 2018, 178: 33-39
14. Iqbal K, Iqbal A, Kirillov A M, Liu W, Tang Y. Hybrid metal-organic-framework/inorganic nanocatalyst toward highly efficient discoloration of organic dyes in aqueous medium. *Inorganic Chemistry*, 2018, 57(21): 13270-13278
15. Qin L, Yi H, Zeng G, Lai C, Huang D, Xu P, Fu Y, He J, Li B, Zhang C. Hierarchical porous carbon material restricted as catalyst for highly catalytic reduction of nitroaromatics. *Journal of Hazardous Materials*, 2019, 380: 120864
16. Ismail M, Khan M I, Khan S B, Akhtar K, Khan M A, Asiri A M. Catalytic reduction of picric acid, nitrophenols and organic azo dyes via green synthesized plant supported Ag nanoparticles. *Journal of Molecular Liquids*, 2018, 268: 87-101
17. Bhaskar R, Joshi H, Sharma A K, Singh, A K. Reusable catalyst for transfer hydrogenation of aldehydes and ketones designed by anchoring palladium as nanoparticles on graphene oxide functionalized with selenated amine. *ACS Applied Materials & Interfaces*, 2017, 9(3): 2223-2231
18. Zhou Y, Liu J, Li X, Pan X, Bao, X. Selectivity modulation in the consecutive hydrogenation of benzaldehyde via functionalization of carbon nanotubes. *Journal of Natural Gas Chemistry*, 2012, 21(3): 241-245
19. Pu C, Zhang J, Chang G, Xiao Y, Ma X, Wu J, Luo T, Huang K, Ke S, Li J, Yang X. Nitrogen precursor-mediated construction of N-doped hierarchically porous carbon-supported Pd catalysts with controllable morphology and composition. *Carbon*, 2020, 159: 451-460
20. Advani J H, Noor-ul H K, Bajaj H C, Biradar A V. Stabilization of palladium nanoparticles on chitosan derived N-doped carbon for hydrogenation of various functional groups. *Applied Surface Science*, 2019, 487: 1307-1315
21. Yang J, Yuan M, Xu D, Zhang H, Zhu Y, Fan M, Zhang F, Dong Z. Highly

dispersed ultrafine palladium nanoparticles encapsulated in a triazinyl functionalized porous organic polymer as a highly efficient catalyst for transfer hydrogenation of aldehydes. *Journal of Materials Chemistry A*, 2018, 6(37): 18242-18251

22. Stucchi M, Vasile F, Cattaneo S, Villa A, Chierigato A, Vandegheuchte B D, Prati L. An Insight into the role of reactant structure effect in Pd/C catalysed aldehyde hydrogenation. *Nanomaterials*, 2022, 12(6): 908
23. Anderson J A, Athawale A, Imrie F E, McKenna F M, McCue A, Molyneux D, Power K, Shand M, Wells R P K. Aqueous phase hydrogenation of substituted phenyls over carbon nanofibre and activated carbon supported Pd. *Journal of Catalysis*, 2010, 270(1): 9-15